Struct Multidisc Optim (2012) 45:693–701
DOI 10.1007/s00158-011-0730-z

RESEARCH PAPER

# Drag minimization and lift maximization in laminar flows via topology optimization employing simple objective function expressions based on body force integration

**Tsuguo Kondoh · Tadayoshi Matsumori · Atsushi Kawamoto**

Received: 1 February 2011 / Revised: 12 October 2011 / Accepted: 14 October 2011 / Published online: 12 November 2011


**Abstract** This paper deals with topology optimization of body shapes in fluid flows, where some new ideas for drag minimization and lift maximization problems are proposed. For drag minimization problems, the objective function is expressed as a body force integration in the flow domain. Also a similar expression of objective function is given for lift maximization problems. Employing those objective function expressions, optimum shapes of bodies in incompressible axisymmetric and two-dimensional flows are numerically investigated.

**Keywords** Topology optimization · Laminar flow · Fluid dynamic drag · Fluid dynamic lift

## 1 Introduction

Borrvall and Petersson (2003) presented a basic idea for topology optimization of fluid related problems, where influence of the wall or the body in fluid on the flow is represented as a body force like the one exerted by the porous media, and the objective function is expressed as total energy dissipated in the flow domain. With this method they obtained optimized geometry for internal flow problems described by the Stokes equation. Thereafter, similar studies have been conducted for the Stokes flow problems including recent ones by Gersborg-Hansen et al. (2005) and Challis and Guest (2009), and also for the Navier-Stokes flow problems at the Reynolds numbers up to around 100, e.g. Olesen et al. (2006).

T. Kondoh (✉) · T. Matsumori · A. Kawamoto
Toyota Central R&D Labs., Nagakute, Aichi 480-1192, Japan
e-mail: tsuguo-kondoh@mosk.tytlabs.co.jp

However, objective function for topology optimization in fluid related problems seems yet to be fully investigated. Adoption of energy dissipation expression (Borrvall and Petersson 2003) is quite natural considering energy conservation in flow domain, and suitable for internal flow problems, but it is not obvious that it can be applied to external flow problems like drag minimization. Moreover for lift maximization problems, there have been no proper expressions of objective function which can be used for topology optimization.

In this paper, some new ideas for drag minimization and lift maximization problems are proposed. For drag minimization problems, the objective function is expressed as a body force integration in the flow domain, which differs from the one usually adopted in minimum energy loss problems. Also a similar expression of objective function is given for lift maximization problems. In addition, an expression for the parameter ($\alpha_{\max}$) accompanying body force term in fluid equation is presented, which can be used without tuning for wide range of the Reynolds number in laminar flow regimes. Employing these objective function and body force expressions, optimum shapes of bodies in incompressible axisymmetric and two-dimensional flows are numerically investigated. All the computations are executed using finite element software package COMSOL Multiphysics.

## 2 Topology optimization for drag minimization and lift maximization

### 2.1 Problem settings

We seek the optimum body shapes in the flow. To do that we first introduce $\gamma = \gamma(\mathbf{x})$ $(0 \leq \gamma \leq 1)$ as the design variable, which represents fluid fraction at arbitrary point $\mathbf{x}$

in the flow domain, i.e., $\gamma = 1$ at the point occupied by pure fluid, $\gamma = 0$ at the pure solid point, and $0 < \gamma < 1$ at the point in intermediate state. The body shape can be expressed as the assembly of the part with $\gamma \leq \epsilon$ where $\epsilon$ is a value very small compared with 1.

Figure 1 shows the problem settings. We consider the flow in the domain $\Omega$ where the equations describing flow field, given in the following section, are to be satisfied. The body can exist only in the design domain $\Omega_{\mathrm{D}}$, a part of $\Omega$, where the design variable $\gamma$ is defined and its distribution is to be optimized. $\Gamma$, the boundary of $\Omega$, consists of the inlet boundary $\Gamma_{\mathrm{in}}$, the outlet boundary $\Gamma_{\mathrm{out}}$ and the lateral boundaries $\Gamma_{\mathrm{lat}}$. The flow velocity $\mathbf{U}$ on $\Gamma_{\mathrm{in}}$ is assumed $x$-directed and uniform ($\mathbf{U} = [U, 0, 0]^{\mathrm{T}}$; usually $\mathbf{U} = [1, 0, 0]^{\mathrm{T}}$ in non-dimensional computations), the pressure $p$ on $\Gamma_{\mathrm{out}}$ is assumed constant ($p = p_0$; usually $p = 0$ in non-dimensional computations), and the open boundary (no viscous stress) condition is assumed on $\Gamma_{\mathrm{lat}}$. We explore the distribution of $\gamma$ in $\Omega_{\mathrm{D}}$ which minimizes the drag force or maximizes the lift force exerted by the flow on the body.

Optimization problems can be formulated, for drag minimization problem e.g., as

$$\underset{\gamma\in[0,1]}{\text{minimize}} \quad J[\gamma] := \int_{\Omega} L(\gamma)\, d\Omega + \int_{\Gamma} \ell(\gamma)\, d\Gamma, \tag{1}$$

$$\text{subject to} \quad G[\gamma] := V - \int_{\Omega} (1-\gamma)\, d\Omega \leq 0. \tag{2}$$

$L$ and $\ell$ are integrands to define the objective function $J$ expressing fluid dynamic drag force, concrete forms of which are given in Section 2.3. $V$ is the lower bound for the volume (in axisymmetric problem) or the section area (in two-dimensional problem) of the body which is to be satisfied in the final result of optimization.

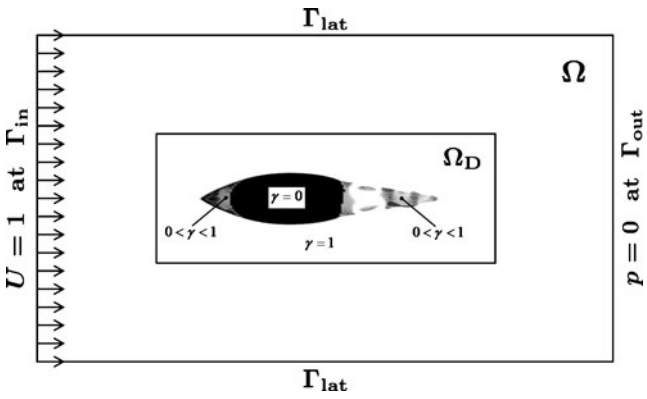


**Fig. 1** Problem settings: Flow equations are solved in domain $\Omega$ surrounded by inlet boundary $\Gamma_{\mathrm{in}}$, outlet boundary $\Gamma_{\mathrm{out}}$ and lateral boundaries $\Gamma_{\mathrm{lat}}$. Design variable $\gamma$ defined as fluid fraction at arbitrary point to describe body shape is to be optimized in domain $\Omega_{\mathrm{D}}$

## 2.2 Equations describing flow field

In this subsection we go through the governing equations for the fluid flow. Also we derive some useful equations to be used in defining relevant objective functions in the following Section 2.3. We start with the following equations, governing steady incompressible Newtonian flows, expressed in terms of velocity vector $\mathbf{u}$ and total stress tensor $\mathbf{P}$ with body force vector $\mathbf{f}$:

$$\nabla \cdot \mathbf{u} = 0, \tag{3}$$

$$\nabla \cdot \left(\mathbf{u}\mathbf{u}^{\mathrm{T}}\right) = \nabla \cdot \mathbf{P} + \mathbf{f}(\mathbf{x}), \tag{4}$$

where the superscript T indicates transpose of vector or tensor, and $\mathbf{u}\mathbf{u}^{\mathrm{T}}$ means the momentum flux tensor. Total stress tensor $\mathbf{P}$ consists of isotropic tensor due to pressure $p$ and viscous stress tensor $\mathbf{T}$:

$$\mathbf{P} = -p\mathbf{I} + \mathbf{T}, \tag{5}$$

$$\mathbf{T} = \frac{1}{\mathrm{Re}} \left\{ \nabla\mathbf{u} + (\nabla\mathbf{u})^{\mathrm{T}} \right\}, \tag{6}$$

where $\mathbf{I}$ is the unit tensor. Note that all the variables are made non-dimensional using the reference length and velocity, $L$ and $U$, and the density of fluid, $\rho$:

$$\frac{\mathbf{x}}{L} \to \mathbf{x}, \quad \frac{\mathbf{u}}{U} \to \mathbf{u}, \quad \frac{p - p_0}{\rho U^2} \to p. \tag{7}$$

As a result, non-dimensional parameter Re, i.e. the Reynolds number defined as

$$\mathrm{Re} \equiv \frac{LU}{\nu}, \tag{8}$$

appears in the governing equations, where $\nu$ is the kinematic viscosity of fluid.

Following Borrvall and Petersson (2003), the influence of a body in fluid on the flow is expressed as a body force $\mathbf{f}(\mathbf{x}) = -\alpha(\mathbf{x})\mathbf{u}(\mathbf{x})$ in (4), where the coefficient $\alpha(\mathbf{x})$ is related to the design variable $\gamma(\mathbf{x})$ as follows:

$$\alpha(\mathbf{x}) = \alpha\left(\gamma(\mathbf{x})\right) = \alpha_{\max} \frac{q\left\{1 - \gamma(\mathbf{x})\right\}}{q + \gamma(\mathbf{x})}. \tag{9}$$

Here $q$ is a positive parameter controlling the shape of function $\alpha(\gamma)$, and is given the value, e.g. 0.1. The parameter $\alpha_{\max}$ should be large enough so that the solution of (4) at

solid part ($\gamma = 0$) substantially yields $\mathbf{u} = \mathbf{0}$. Then we express $\alpha_{\max}$ as

$$\alpha_{\max} = \left(1 + \frac{1}{\mathrm{Re}}\right)\chi, \tag{10}$$

and set $\chi$ with a value much larger than 1, e.g. $10^4$. This ensures that $\alpha_{\max}$ is superior to any other coefficient in (4) by factor $\chi$ regardless of Re.

The conservation law of kinetic energy of fluid is obtained by taking dot product of $\mathbf{u}$ and (4) as

$$\nabla \cdot \left(\mathbf{u}\frac{\mathbf{u}^2}{2}\right) = \nabla \cdot \left(\mathbf{P}^{\mathrm{T}}\mathbf{u}\right) - \Phi + \mathbf{f}(\mathbf{x}) \cdot \mathbf{u}, \tag{11}$$

where $\Phi$ is the energy dissipated in the flow due to viscosity per unit time and volume:

$$\Phi \equiv \mathbf{T} : \nabla\mathbf{u} = \frac{1}{2\mathrm{Re}}\left\{\nabla\mathbf{u} + (\nabla\mathbf{u})^{\mathrm{T}}\right\}^2. \tag{12}$$

It is useful to derive conservation laws in whole flow domain $\Omega$, which are obtained by integrating (3), (4) and (11) in $\Omega$ as

$$\int_\Gamma \mathbf{u} \cdot \mathbf{n}\, d\Gamma = 0, \tag{13}$$

$$\int_\Gamma \mathbf{u}\,(\mathbf{u} \cdot \mathbf{n})\, d\Gamma = \int_\Gamma \boldsymbol{\sigma}\, d\Gamma + \int_\Omega \mathbf{f} d\Omega, \tag{14}$$

$$\int_\Gamma \left(p + \frac{\mathbf{u}^2}{2}\right)(\mathbf{u} \cdot \mathbf{n})\, d\Gamma = \int_\Gamma (\boldsymbol{\tau} \cdot \mathbf{u})\, d\Gamma + \int_\Omega \{\mathbf{f} \cdot \mathbf{u} - \Phi\}\, d\Omega, \tag{15}$$

where $\boldsymbol{\sigma} = \mathbf{Pn} = -p\mathbf{n} + \boldsymbol{\tau}$ and $\boldsymbol{\tau} = \mathbf{Tn}$ are total and viscous stress vectors, and $\mathbf{n}$ is the unit outward normal vector on the boundary $\Gamma$ of flow domain $\Omega$.

In addition, we prepare supplementary equations which are to be used in next subsection for expressing objective functions. We take dot product of an arbitrary constant vector $\mathbf{V}$ and (14) as

$$\int_\Gamma (\mathbf{u} \cdot \mathbf{V})(\mathbf{u} \cdot \mathbf{n})\, d\Gamma = \int_\Gamma \boldsymbol{\sigma} \cdot \mathbf{V}\, d\Gamma + \mathbf{V} \cdot \int_\Omega \mathbf{f} d\Omega, \tag{16}$$

which is converted to

$$\begin{aligned}\mathbf{V} \cdot \int_\Omega \mathbf{f} d\Omega &= \frac{1}{2}\int_\Gamma \left\{\mathbf{u}^2 + \mathbf{V}^2 - (\mathbf{u} - \mathbf{V})^2\right\}(\mathbf{u} \cdot \mathbf{n})\, d\Gamma \\ &\quad + \int_\Gamma \boldsymbol{\sigma} \cdot (\mathbf{u} - \mathbf{V})\, d\Gamma - \int_\Gamma (-p\mathbf{n} + \boldsymbol{\tau}) \cdot \mathbf{u}\, d\Gamma \\ &= \int_\Gamma \left\{\left(p + \frac{\mathbf{u}^2}{2}\right)(\mathbf{u} \cdot \mathbf{n}) - \boldsymbol{\tau} \cdot \mathbf{u} + \boldsymbol{\sigma} \cdot (\mathbf{u} - \mathbf{V}) \right. \\ &\quad \left. - \frac{1}{2}(\mathbf{u} - \mathbf{V})^2 (\mathbf{u} \cdot \mathbf{n})\right\} d\Gamma, \end{aligned} \tag{17}$$

where (13) is applied. We can also rewrite this equation, by using (15), as

$$\begin{aligned}\mathbf{V} \cdot \int_\Omega \mathbf{f} d\Omega &= \int_\Omega \{\mathbf{f} \cdot \mathbf{u} - \Phi\}\, d\Omega \\ &\quad + \int_\Gamma \left\{\boldsymbol{\sigma} \cdot (\mathbf{u} - \mathbf{V}) - \frac{1}{2}(\mathbf{u} - \mathbf{V})^2 (\mathbf{u} \cdot \mathbf{n})\right\} d\Gamma. \end{aligned} \tag{18}$$

### 2.3 Objective functions

This subsection presents several possible expressions of the objective function regarding drag minimization and lift maximization. We consider the external flow with uniform far-away velocity $\mathbf{U} = [U, 0, 0]^{\mathrm{T}}$ flowing around isolated body. Under this circumstance, fluid force is usually expressed as integration of stress vector $\boldsymbol{\sigma}$ on body surface, but it is not suited for topology optimization because the body shape is not known in advance. In our formulation, the influence of the body is expressed as a body force $\mathbf{f}$ in momentum (4), then the force $\mathbf{F}$ exerted by the flow on the body should be expressed as domain integration of $-\mathbf{f}$ due to the action-reaction law, i.e.,

$$\mathbf{F} = -\int_\Omega \mathbf{f} d\Omega = \int_\Omega \alpha\mathbf{u}\, d\Omega. \tag{19}$$

Or, this can be rewritten, based on momentum conservation law (14), as

$$\mathbf{F} = -\int_\Omega \mathbf{f} d\Omega = \int_\Gamma \{-\mathbf{u}\,(\mathbf{u} \cdot \mathbf{n}) + \boldsymbol{\sigma}\}\, d\Gamma, \tag{20}$$

which means the momentum loss occurs in the flow domain $\Omega$ by the amount of total force exerted by the flow, i.e., body force integration in $\Omega$ and surface force integration on $\Gamma$. The right-hand side of this equation is naturally the same as the one derived when $\mathbf{F}$ is expressed as integration of stress vector $\boldsymbol{\sigma}$ on body surface.

For another interpretation of (19), we divide the flow domain $\Omega$ into two parts, i.e., pure-fluid part $\Omega_F$ ($\gamma = 1$, $\mathbf{f} = \mathbf{0}$) and quasi-solid part $\Omega_{S^*}$ ($0 \le \gamma < 1$, $\mathbf{f} \neq \mathbf{0}$), and rewrite (19) with $\mathbf{f}$ replaced with $-\nabla \cdot \left(\mathbf{P} - \mathbf{uu}^{\mathrm{T}}\right)$ due to the momentum equation (4) as

$$\begin{aligned}\mathbf{F} &= -\int_\Omega \mathbf{f} d\Omega = -\int_{\Omega_{S^*}} \mathbf{f} d\Omega \\ &= \int_{\Omega_{S^*}} \left\{\nabla \cdot \left(\mathbf{P} - \mathbf{uu}^{\mathrm{T}}\right)\right\} d\Omega \\ &= \int_{\Gamma_{S^*}} \{\boldsymbol{\sigma} - \mathbf{u}\,(\mathbf{u} \cdot \mathbf{n})\}\, d\Gamma \approx \int_{\Gamma_{S^*}} \boldsymbol{\sigma}\, d\Gamma, \end{aligned} \tag{21}$$

where the velocity on $\Gamma_{S^*}$, the surface of quasi-solid part $\Omega_{S^*}$, is assumed to be quite small ($\mathbf{u} \approx \mathbf{0}$) because $\Gamma_{S^*}$

is almost the same as the body surface. This expression of fluid force is substantially equivalent to the normally used one, i.e., integration of stress vector $\boldsymbol{\sigma}$ on body surface. This again justifies the fluid force expression (19).

Thus fluid dynamic drag $D$ can be expressed as $x$-component of (19) as

$$D = \int_\Omega \alpha u \, d\Omega \equiv J_1, \tag{22}$$

where $u$ is $x$-component of velocity vector $\mathbf{u}$. It gives a quite simple expression in the domain integration form that is suitable for topology optimization.

There are also other expressions for drag $D$. First an expression in boundary integration form is obtained from $x$-component of (20), i.e.,

$$D = \int_\Gamma \{-u\,(\mathbf{u}\cdot\mathbf{n}) - p n_x + \tau_x\}\, d\Gamma \equiv J_{2a}, \tag{23}$$

where $n_x$ and $\tau_x$ are $x$-components of vectors $\mathbf{n}$ and $\boldsymbol{\tau}$. Furthermore, the other expressions are obtained from supplementary (17) and (18) prepared in the previous subsection. In these equations, we replace $\mathbf{V}$ with uniform far-away velocity $\mathbf{U} = [U, 0, 0]^{\mathrm{T}}$, substitute $-\alpha\mathbf{u}$ for $\mathbf{f}$, and divide the equations by $U$, that yields the following expressions for drag $D$; i.e., an expression in boundary integration form from (17),

$$D = \frac{1}{U}\left[\int_\Gamma \left\{-\left(p + \frac{\mathbf{u}^2}{2}\right)(\mathbf{u}\cdot\mathbf{n}) + \boldsymbol{\tau}\cdot\mathbf{u} - \boldsymbol{\sigma}\cdot(\mathbf{u}-\mathbf{U}) + \frac{1}{2}(\mathbf{u}-\mathbf{U})^2(\mathbf{u}\cdot\mathbf{n})\right\} d\Gamma\right] \equiv J_{3a}, \tag{24}$$

and an expression in domain-boundary mixed integration form from (18),

$$D = \frac{1}{U}\left[\int_\Omega \left(\Phi + \alpha\mathbf{u}^2\right) d\Omega - \int_\Gamma \left\{\boldsymbol{\sigma}\cdot(\mathbf{u}-\mathbf{U}) - \frac{1}{2}(\mathbf{u}-\mathbf{U})^2(\mathbf{u}\cdot\mathbf{n})\right\} d\Gamma\right] \equiv J_{4a}. \tag{25}$$

When the boundary $\Gamma$ is located far away from the body, the velocity $\mathbf{u}$ on $\Gamma$ can be assumed to be approximately equal to the uniform velocity $\mathbf{U}$, and viscous stress $\boldsymbol{\tau}$ on $\Gamma$ would be small enough to be neglected, then the simplified versions of the above equations (23)–(25) are derived:

$$D \approx -\int_\Gamma \{u\,(\mathbf{u}\cdot\mathbf{n}) + p n_x\}\, d\Gamma \equiv J_{2b}, \tag{26}$$

$$D \approx -\frac{1}{U}\left\{\int_\Gamma \left(p + \frac{\mathbf{u}^2}{2}\right)(\mathbf{u}\cdot\mathbf{n})\, d\Gamma\right\} \equiv J_{3b}, \tag{27}$$

$$D \approx \frac{1}{U}\left\{\int_\Omega \left(\Phi + \alpha\mathbf{u}^2\right) d\Omega\right\} \equiv J_{4b}. \tag{28}$$

Now we have various (22)–(28) to express drag force $D$. For drag minimization problems, one can select any of the right-hand sides of them as the objective function $J$:

$$J = \text{one of } \{J_1,\ J_{2a},\ J_{2b},\ J_{3a},\ J_{3b},\ J_{4a},\ J_{4b}\}. \tag{29}$$

Although some of these expressions include a coefficient $1/U$, it can be omitted because $U$ is usually 1 in non-dimensional computations. Note that some are expressed in domain integration form and the others are in boundary integration form.

It should also be noted that the expression (28) without the coefficient $1/U$ is identical with the objective function adopted for minimum energy loss problems in Borrvall and Petersson (2003). It is a natural consequence if we consider, instead of an object placed in flow with uniform far-away velocity $U$, an object moving with constant velocity $U$ in quiet fluid in infinite domain, because in this situation the work done by the moving object, $DU$, balances with the energy dissipated in the whole flow domain, $\int \left(\Phi + \alpha\mathbf{u}^2\right) d\Omega$.

In fact, all the objective functions expressing drag force are exactly or substantially identical from theoretical point of view.

$$J_1 = J_{2a} = J_{3a} = J_{4a} \approx J_{2b} \approx J_{3b} \approx J_{4b}. \tag{30}$$

So the optimized results of computations with them should also be identical. This is demonstrated in Fig. 2 and Table 1, where the computational results of optimization with the four kinds of objective function expressions, $J_1$, $J_{2b}$, $J_{3b}$ and $J_{4b}$, are given for a two-dimensional drag minimization problem at the Reynolds number $\mathrm{Re} = 10$. The details of computational conditions are described in the following Section 3 and not mentioned here. As shown in Fig. 2 and Table 1, both the section profiles and the drag forces of optimized results are substantially identical. Thus it is confirmed that we can use any of them, among which we employ $J_1$ as the objective function for the drag minimization computations in the following Section 3 because it is new and simple, and moreover it leads to an analogous expression for the lift maximization problems as shown in the following paragraph.

Equation (19) expresses vector force exerted by the flow on the body, which contains not only drag force but also lift force. This means that fluid dynamic lift $Y$ can be expressed as $y$-component of (19) as

$$Y = \int_\Omega \alpha v \, d\Omega \equiv K_1, \tag{31}$$

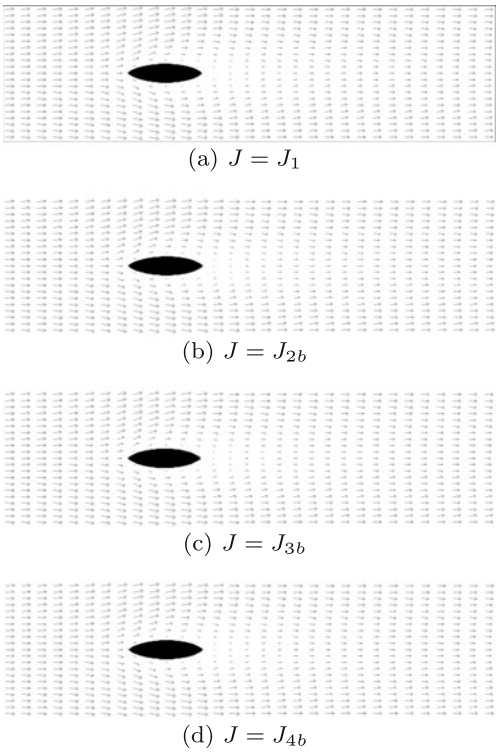

(a) $J = J_1$

(b) $J = J_{2b}$

(c) $J = J_{3b}$

(d) $J = J_{4b}$

**Fig. 2** Section profiles of two-dimensional cylindrical body with minimum drag under constant area constraint for Reynolds number Re = 10: difference due to expression of objective function $J$

where $v$ is $y$-component of velocity vector $\mathbf{u}$. This expression in domain integration form is also quite simple, and is suitable for topology optimization. Expression for $Y$ in boundary integration form is obtained as $y$-component of (20) as

$$Y = \int_\Gamma \left\{ -v\,(\mathbf{u}\cdot\mathbf{n}) - pn_y + \tau_y \right\} d\Gamma \equiv K_{2a}, \tag{32}$$

where $n_y$ and $\tau_y$ are $y$-components of vectors $\mathbf{n}$ and $\boldsymbol{\tau}$. This equation can be approximated when the boundary $\Gamma$ is located far away from the body as

$$Y \approx -\int_\Gamma \left\{ v\,(\mathbf{u}\cdot\mathbf{n}) + pn_y \right\} d\Gamma \equiv K_{2b}. \tag{33}$$

For lift maximization problems, one can select either of the above expressions as the objective function $J$:

$$J = \text{one of } \{-K_1,\ -K_{2a},\ -K_{2b}\}. \tag{34}$$

**Table 1** Drag coefficient of two-dimensional cylindrical body with minimum drag under constant area constraint for Reynolds number Re = 10: difference due to expression of objective function $J$.

| Expression | $J = J_1$ | $J = J_{2b}$ | $J = J_{3b}$ | $J = J_{4b}$ |
|---|---|---|---|---|
| $C_D$ | 2.685 | 2.687 | 2.689 | 2.687 |

Among them we employ $-K_1$, which is analogous to $J_1$, for the lift maximization computations in the following Section 3. Although not treated in the following examples, we can also express an objective function $J$ for maximizing lift-to-drag ratio by simply taking the ratio of $Y$ to $D$ as

$$J = -\frac{Y}{D} = -\frac{\int_\Omega \alpha v\, d\Omega}{\int_\Omega \alpha u\, d\Omega}. \tag{35}$$

### 2.4 Solution procedures

Optimization problems are formulated as (1) and (2), where the objective function $J$ is set as one of the expressions described in the preceding Section 2.3. Then the solution procedures to obtain the body shape which minimizes the drag force or maximizes the lift force exerted by the flow on the body are as follows.

1. Assume the initial guess for the distribution of the design variable $\gamma$ in $\Omega_D$. For example, a circular cylinder with unit area placed at the origin is assumed as initial body shape in two-dimensional drag minimization problem.
2. Solve the equations describing the flow field (3)–(6) to obtain the distributions of the velocity $\mathbf{u}$ and the pressure $p$.
3. Evaluate the sensitivity of the objective function $J$ to the design variable $\gamma$, $\delta J/\delta\gamma$, by the adjoint variable method in discrete form (Olesen et al. 2006).
4. Update the distribution of $\gamma$, based on the sensitivity $\delta J/\delta\gamma$, by the SQP algorithm (Gill 2002).
5. Return to 2, or terminate the procedures if the KKT condition is fulfilled.

All the above procedures were implemented on COMSOL Multiphysics, finite element software package equipped with adjoint-based sensitivity analysis and SQP-based optimization, SNOPT.

## 3 Investigation of optimum shapes of bodies in laminar flows

### 3.1 Minimization of drag in axisymmetric flows

For axisymmetric bodies placed in uniform flow with velocity $U = 1$ (in non-dimensional computations) in $x$ direction, we investigate the profiles (shapes on the meridional plane) of bodies with minimum drag. We employ the objective function $J = J_1$, where $J_1$ is defined in (22), and apply the constraint that the volume of the body is lower-bounded

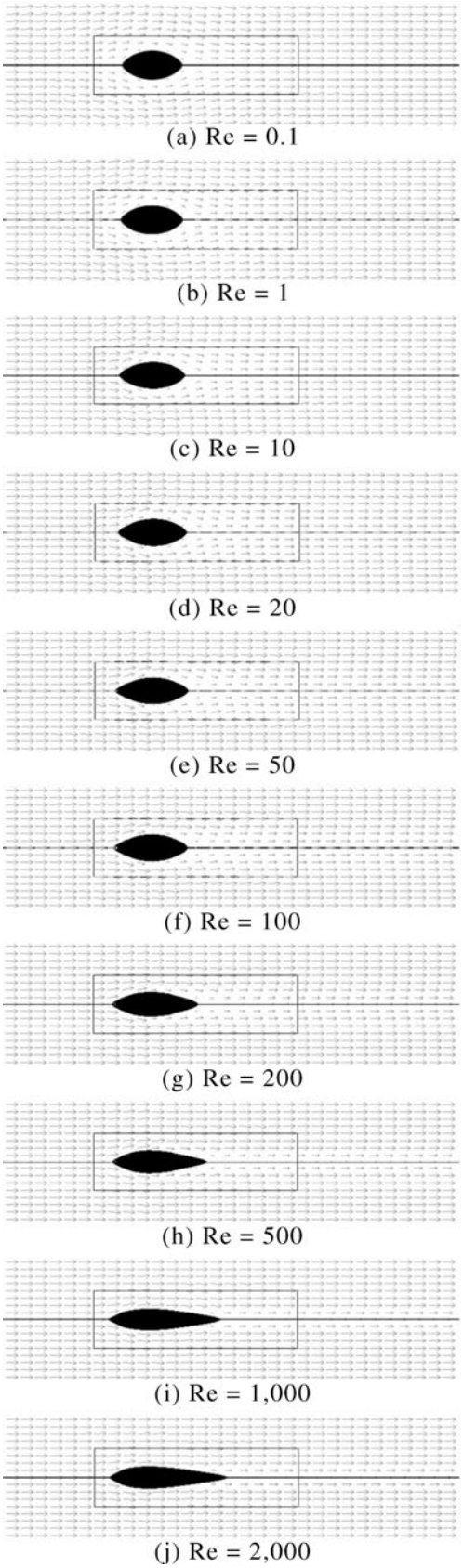


**Fig. 3** Meridional profiles of axisymmetric body with minimum drag for various Reynolds numbers under constant volume constraint

**Table 2** Drag coefficient of axisymmetric body with minimum drag for various Reynolds numbers under constant volume constraint.

| Re | 0.1 | 1 | 10 | 20 | 50 | 100 | 200 | 500 | 1,000 | 2,000 |
|---|---|---|---|---|---|---|---|---|---|---|
| $C_D$ | 230 | 25.5 | 3.96 | 2.42 | 1.30 | 0.83 | 0.55 | 0.32 | 0.21 | 0.14 |

by $V$. We also apply the constraint that the center of gravity of the body is fixed at the origin so that the body location is anchored during the process of optimization. We define the reference length $L$ as $L = V^{1/3}$. Then the Reynolds number Re and the drag coefficient $C_D$ (non-dimensional value of drag force $D^*$) are defined as $\mathrm{Re} \equiv UV^{1/3}/\nu$ and $C_D \equiv 2D^*/(\rho U^2 V^{2/3}) = 2D$.

The results of drag minimization for various Re are presented in Fig. 3 and Table 2. When Re is less than approximately 100, the optimized bodies have the profiles which are almost symmetric laterally and pointed at both the leading and the trailing edges. As Re becomes smaller they become thicker. But for $\mathrm{Re} \lessapprox 1$, they have substantially the same profile of rugby-ball shape with the cone angle at both edges around 120°. When Re becomes greater than 100, the symmetry in the shape disappears and the profiles are laterally extended with Re especially in downstream direction, changing to the so-called streamlined shapes. Both edges are more pointed, and the cone angles become smaller with increasing Re.

It is difficult to verify the results of drag minimization for the Navier-Stokes flows. But for the Stokes flow problem, which correspond to the limit of $\mathrm{Re} \to 0$, theoretical prediction of minimum drag shape in axisymmetric condition is given by Pironneau (1973). Then we treated the same problem and compared the result with Pironneau's prediction. Our result is shown in Fig. 4, which is almost identical to Pironneau's prediction, including that the cone angle at both edges is 120°. In fact, optimized profiles for Navier-Stokes flow shown in Fig. 3 at very low Reynolds number,

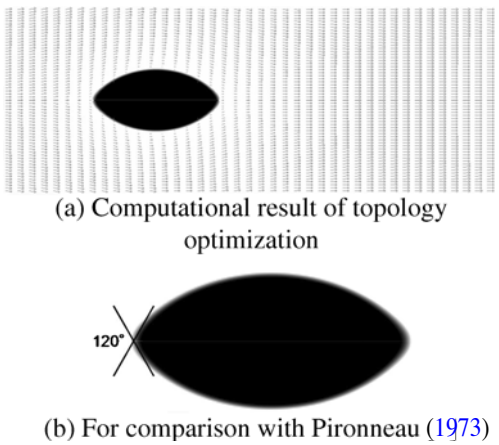


**Fig. 4** Axisymmetric body with minimum drag in Stokes flow under constant volume constraint

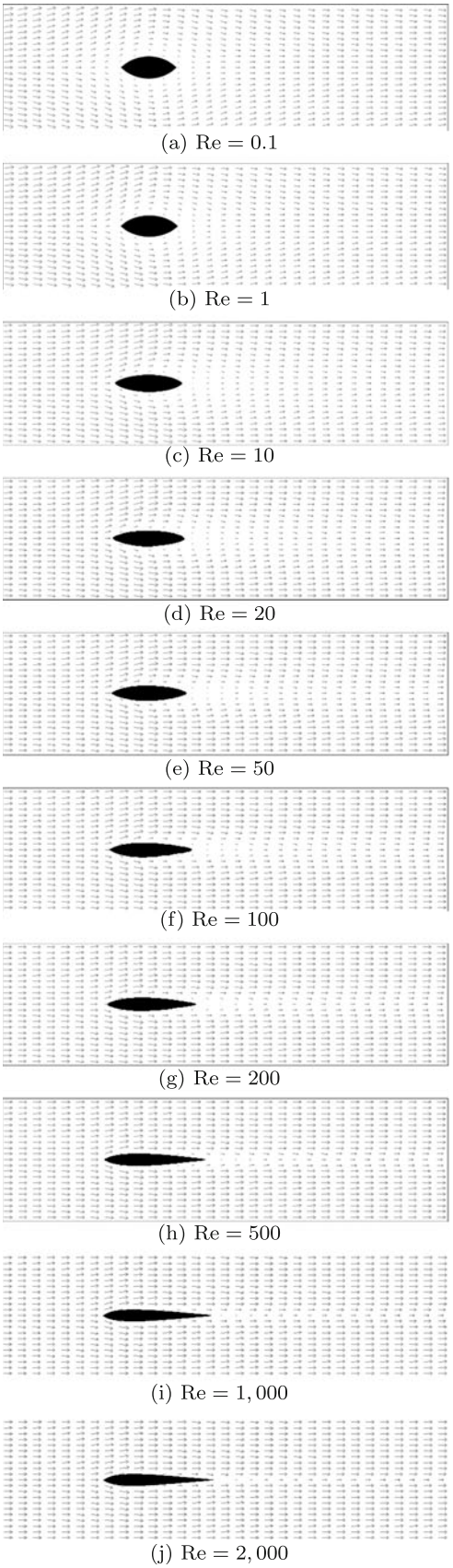


**Fig. 5** Section profiles of two-dimensional cylindrical body with minimum drag for various Reynolds numbers under constant area constraint

Re $\lessapprox$ 1, are also substantially identical to the result for the Stokes flow problem.

### 3.2 Minimization of drag in two-dimensional flows

For two-dimensional bodies placed in uniform flow with velocity $U = 1$ in $x$ direction, we investigate the profiles (section shapes) of bodies with minimum drag. The computational conditions are the same as the axisymmetric cases, except we apply the constraint that the section area, instead of the volume, of the body is lower-bounded by $A$. We define the reference length $L$ as $L = \sqrt{A}$. Then the Reynolds number Re and the drag coefficient $C_{\mathrm{D}}$ are defined as $\mathrm{Re} \equiv U\sqrt{A}/\nu$ and $C_{\mathrm{D}} \equiv 2D^*/(\rho U^2 A) = 2D$, respectively.

The results of drag minimization for various Re are presented in Fig. 5 and Table 3. The way that the profiles change with Re is qualitatively the same as the axisymmetric cases, although the thickness-length ratio in the profiles seems smaller. It may be worth noting that, for very low Reynolds number, Re $\lessapprox$ 1, the minimum drag bodies have almost the same profiles. In addition, the wedge angle at both edges is around 90°, which is consistent with the suggestion by Pironneau (1974).

### 3.3 Maximization of lift in two-dimensional flows

We investigate the profiles (section shapes) of two-dimensional bodies with maximum lift in uniform flow with velocity $U = 1$ in $x$ direction. We employ the objective function $J = -K_1$, where $K_1$ is defined in (31). The other computational conditions follow the drag-minimization problems. Besides, we apply additional constraint on drag, i.e., $C_{\mathrm{D}}/C_{\mathrm{Dmin}} \leq \beta$, where $C_{\mathrm{Dmin}}$ is the minimum drag at specified Re, and $\beta$ is the coefficient on upper limit of drag force. This additional constraint is necessary because lift can be made unlimitedly large, e.g. by making the thickness of inclined plate extremely thin while keeping the section area $A$ constant.

The results of lift maximization at the Reynolds number Re = 10 for $\beta = \{1.1,\ 1.2,\ 1.5,\ 2\}$ are presented in Fig. 6 and Table 4. The minimum drag at Re = 10 is $C_{\mathrm{Dmin}} = 2.69$ as given in Table 3. The lift coefficient $C_{\mathrm{L}}$ (non-dimensional value of lift force $Y^*$) is defined as $C_{\mathrm{L}} \equiv 2Y^*/(\rho U^2 A) = 2Y$. The computations are started with the minimum drag

**Table 3** Drag coefficient of two-dimensional cylindrical body with minimum drag for various Reynolds numbers under constant area constraint.

| Re | 0.1 | 1 | 10 | 20 | 50 | 100 | 200 | 500 | 1,000 | 2,000 |
|---|---|---|---|---|---|---|---|---|---|---|
| $C_{\mathrm{D}}$ | 90.8 | 12.1 | 2.69 | 1.81 | 1.10 | 0.76 | 0.53 | 0.33 | 0.22 | 0.15 |

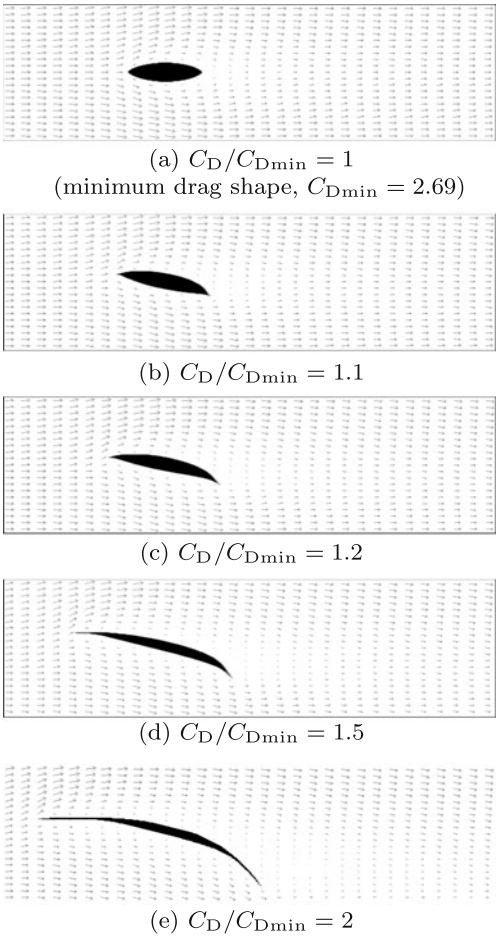


**Fig. 6** Section profiles of two-dimensional cylindrical body with maximum lift under constant area and upper bounded drag constraints for Re = 10

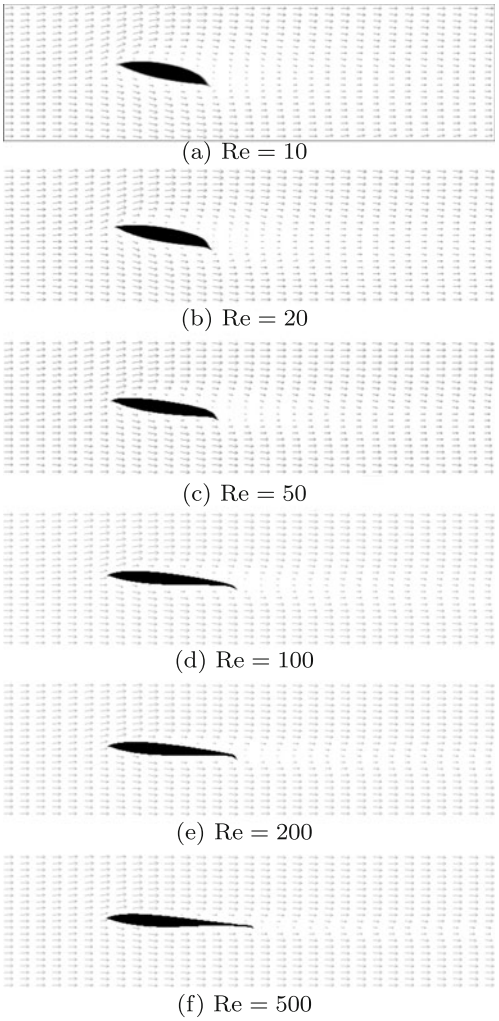


**Fig. 7** Section profiles of two-dimensional cylindrical body with maximum lift for various Reynolds numbers under constant area constraint and upper bounded drag constraint $C_D/C_{Dmin} \leq 1.1$

shape shown in Fig. 6(a), which is identical to Fig. 5(c), to seek the optimized shape for $\beta = 1.1$. The result is an inclined profile as shown in Fig. 6(b), where the lower surface is planarized and becomes slightly convex upward near the leading and the trailing edges. Then with this result as initial condition, optimized shape for $\beta = 1.2$ is obtained, and subsequently for $\beta = 1.5$ and $\beta = 2$. In the result for $\beta = 1.2$ shown in Fig. 6(c), the lower surface of the body is more planarized, the upper surface near the leading edge becomes almost parallel to the main stream, and the trailing edge bends downward with sharply pointed end. In the results for $\beta = 1.5$ and $\beta = 2$ shown in Fig. 6(d) and (e), these features on the profiles are more pronounced.

The results of lift maximization at larger Reynolds numbers Re = {20, 50, 100 200, 500} for $\beta = 1.1$ are presented in Fig. 7 and Table 5. As shown in Fig. 7, the optimized bodies have the profiles which change considerably with Re. As Re becomes larger, the profiles extend laterally,

**Table 4** Lift coefficient $C_L$ and lift-to-drag ratio $C_L/C_D$ of two-dimensional cylindrical body with maximum lift under constant area and upper bounded drag constraints for Re = 10.

| $C_D/C_{Dmin}$ | 1 | 1.1 | 1.2 | 1.5 | 2 |
|---|---|---|---|---|---|
| $C_L$ | 0 | 1.89 | 2.84 | 5.27 | 8.72 |
| $C_L/C_D$ | 0 | 0.64 | 0.88 | 1.31 | 1.62 |

**Table 5** Lift coefficient $C_L$ and lift-to-drag ratio $C_L/C_D$ of two-dimensional cylindrical body with maximum lift for various Reynolds numbers under constant area constraint and upper bounded drag constraint $C_D/C_{Dmin} \leq 1.1$.

| Re | 10 | 20 | 50 | 100 | 200 | 500 |
|---|---|---|---|---|---|---|
| $C_L$ | 1.89 | 1.87 | 1.74 | 1.65 | 1.55 | 1.34 |
| $C_L/C_D$ | 0.64 | 0.94 | 1.4 | 2.0 | 2.7 | 3.7 |

mainly in the downstream direction, making their trailing edges pointed very sharply. It is interesting that the profiles for larger Re's bend rapidly near the trailing edge. Although more precise investigation is needed, this possibly suggests the usefulness of flap-like structure at the trailing edge. The thickness of the profiles becomes thinner with increasing Re though the amount of change is small. The angle of inclination of the profiles or the attack angle becomes gradually smaller with increasing Re. The lift coefficient $C_{\mathrm{L}}$ decreases, but the lift-to-drag ratio $C_{\mathrm{L}}/C_{\mathrm{D}}$ increases with increasing Re as shown in Table 5.

## 4 Conclusions

Some new ideas on topology optimization for flow related problems are proposed, in which main items are:

1. For both drag minimization and lift maximization problems, the objective function can be simply expressed as integration of body force in flow domain.
2. Regarding the parameter $\alpha_{\max}$ accompanying body force term in fluid equation, by expressing it as (10) depending on the Reynolds number Re, we can make it applicable without any more tuning to wide range of Re in laminar flow regimes including very low Re.

Employing these objective function and body force expressions, optimum shapes of bodies in incompressible axisymmetric and two-dimensional flows have been numerically investigated, where minimum drag shapes of axisymmetric and two-dimensional bodies for Re up to 2,000 are obtained under constant volume or section area constraint, and maximum lift shapes of two-dimensional bodies for Re up to 500 under constant area and upper bounded drag constraints.

## References

Borrvall T, Petersson J (2003) Topology optimization of fluids in Stokes flow. Int J Numer Methods Fluids 41:77–107

Gersborg-Hansen A, Sigmund O, Haber RB (2005) Topology optimization of channel flow problems. Struct Multidisc Optim 30(3):181–192

Challis VJ, Guest JK (2009) Level set topology optimization of fluids in Stokes flow. Int J Numer Methods Eng 79:1284–1308

Olesen LH, Okkels F, Bruus H (2006) A high-level programming-language implementation of topology optimization applied to steady-state Navier-Stokes flow. Int J Numer Methods Eng 65(7):975–1001

Gill PE (2002) SNOPT: an SQP algorithm for large-scale constrained optimization. SIAM J Optim 12(4):979–1006

Pironneau O (1973) On optimum profiles in Stokes flow. J Fluid Mech 59:117–128

Pironneau O (1974) On optimum design in fluid mechanics. J Fluid Mech 64:97–110